Supporting Information

Cu-based Dual-Metal Site Catalysts for Efficient Alkaline Hydrogen Evolution Reaction

Jingwei Li,[a,b] Tiantian Yang,[a,b] Nana Zhang,[a,b] Linjie Zhang,[a,b] Rui Zhang,[a,b] Jing Yang,[a,b] Cunku Dong,[a,b] Pengfei Yin,[a,b] Hui Liu,*[a,b] Xi-Wen Du[a,b]

Synthesis of $CuRh_1Cr_1$ DMSC Catalyst and Comparative Samples

Two copper targets (with a diameter of 5 cm and a purity of 99.9%) were mechanically polished and ultrasonically cleaned in ultrapure water for 15 minutes. A 200 mL aqueous solution containing 0.5 mol/L $RhCl_3·3H_2O$ (Maisike Chemical Co.) and 0.1 mol/L $CrCl_3·6H_2O$ (Sigma-Aldrich, 99%) was prepared as the electrolyte. One target was immersed in the electrolyte as the cathode within a 1 L metal container, while the other was connected to an electric spark machine as the anode. Spark ablation in liquid was conducted at 298 K (controlled by a cooling bath) for 20 min under the following parameters: current 10 A, pulse width 50 µs, interval 100 µs (duty cycle 33%). The scolloidal product was centrifuged and washed four times using a high-speed centrifuge (18,000 rpm, 12 minutes, SIGMA 3K30), and lyophilized (Biocool-FD-1-50, -50°C pre-freezing, 20 Pa, 16 h) to obtain $CuRh_1Cr_1$ DMSC. The powder was reduced in a tube furnace under 10% H_2/He (50 sccm) at 573 K (5 K/min ramp) for 4 h. For $CuRh_1$ MSC and $CuCr_1$ MSC, identical procedures were followed using 0.5 mol/L $RhCl_3·3H_2O$ or 0.5 mol/L $CrCl_3·6H_2O$ as the sole electrolyte, respectively. The final powder (3 mg) was mixed with carbon black (Sigma-Aldrich, 5mg) for HER testing.

Material Characterization

Transmission electron microscopy (TEM) and energy-dispersive X-ray spectroscopy (EDX) elemental mapping were performed using a JEOL JEM-F200 transmission electron microscope. Scanning electron microscopy (SEM) characterization was conducted on a Hitachi S-4800 scanning electron microscope. High-angle annular dark-field scanning transmission electron microscopy (HAADF-STEM) analysis was performed on an FEI Titan Cubed Themis G2 300 operated at 200 kV. Catalyst concentrations were quantified via inductively coupled plasma mass spectrometry (ICP-MS, Agilent 7700x). X-ray photoelectron spectroscopy (XPS) measurements were carried out on an ESCALAB-250Xi spectrometer equipped with an Al Kα X-ray source (spot size: 650 µm) under standard lens mode, with binding energies calibrated to the C 1s peak at 284.8 eV. Powder X-ray diffraction (XRD) patterns of the prepared samples were recorded on a Bruker D8 Advanced diffractometer using Cu Kα radiation. Raman spectra were collected on a Horiba Labram HR Evolution system with a 532 nm excitation wavelength. In situ Raman spectra were obtained after 10-minute reduction at various potentials in a 1 M KOH aqueous solution. In situ infrared spectra were acquired using a FEI iS50 spectrometer following 10-minute reduction at different potentials in a 1 M KOH aqueous solution.

Electrochemical Measurements

Electrochemical measurements were performed at room temperature using a three-electrode electrochemical cell system on a CHI 660E electrochemical workstation (CH Instruments, Shanghai). A graphite rod was used as the counter electrode, a saturated calomel electrode (SCE) as the reference electrode, and a modified glassy carbon electrode (GCE, d = 5 mm) as the working electrode. Typically, 3 mg of catalyst powder and 5mg of carbon black was dispersed in 500 µL of a mixed solution of water and ethanol (1:1, v/v), followed by the addition of 20 µL of Nafion solution (5 wt% in water). The suspension was sonicated for 30 minutes to prepare a homogeneous ink. The working electrode was prepared by depositing 10 µL of the catalyst ink onto the GCE with a diameter of 5 millimeters. HER electrochemical measurements were conducted in 1 M KOH (pH = 14). Cyclic voltammetry (CV) was performed at a scan rate of 50 mV/s, and linear sweep voltammetry (LSV) was conducted at a scan rate of 5 $mV\cdot s^{-1}$ in 1 M KOH solution. All LSV measurements were performed with 100% iR compensation, and the measured current densities were normalized to the geometric area of the working electrode (0.1963 cm^2). Stability tests were carried out using chronoamperometry without iR correction. Electrochemical impedance spectroscopy (EIS) data were recorded within a frequency range of 0.1–10^5 kHz at an overpotential of 10 mA cm^{-2}. The electrochemical active surface area (ECSA) was calculated from the electrochemical double-layer capacitance of the catalytic surface. The double-layer capacitance (Cdl) of the catalysts was estimated by performing CV in the potential range of 0.57 to 0.67 V vs RHE (non-Faradaic potential range) at different scan rates (20, 40, 60, 80, and 100 mV s^{-1}), followed by extracting the slope from the resulting |ja-jc|/2 vs v plots (ja and jc represent the anodic and cathodic currents at 0.1475 V vs RHE). All potentials were calculated with respect to the reversible hydrogen electrode (RHE) scale according to the Nernst equation (ERHE = ESCE + 0.0591 × pH + 0.241 V at 298 K).

The synthesis process of $CuRh_1Cr_1$ DMSC

The synthesis process of $CuRh_1Cr_1$ DMSC via the SAL method was illustrated in Figure S1. Firstly, an aqueous solution containing Rh and Cr ions was placed between the Cu cathode and anode. During the spark discharge cycle, the cathode and anode were gradually approaching each other in the aqueous solution. When the distance achieved to a critical point, the solution was first ionized then heated the Cu anode to form Cu plasma. The two types of plasma mixed immediately. After the discharge, the mixed plasma condensed, enabling Rh and Cr atoms to be co-doped into the Cu nanoparticle. By adjusting the concentration of Rh and Cr ions in the aqueous solution, $CuRh_1Cr_1$ DMSC was obtained. Finally, a thermal hydrogen reduction treatment was applied to eliminate the surface oxides of $CuRh_1Cr_1$ DMSC. For comparison, the $CuRh_1$ MSC and $CuCr_1$ MSC samples were synthesized under identical conditions, using solutions containing only Rh^{3+} or Cr^{3+} ions.

Results and Discussion

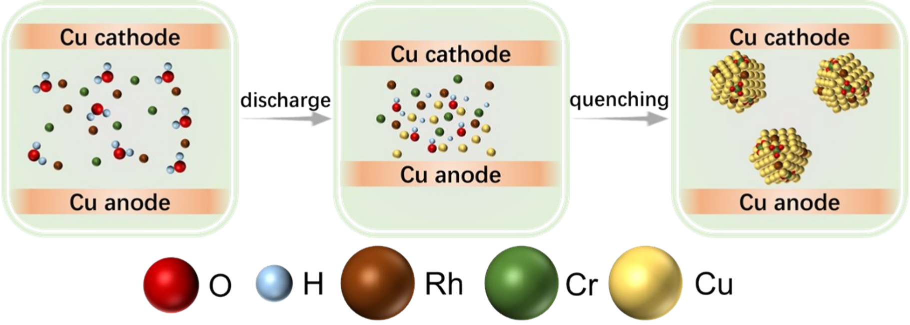

Figure S1 Schematic illustration of the synthetic procedure for $CuRh_1Cr_1$ DMSC.

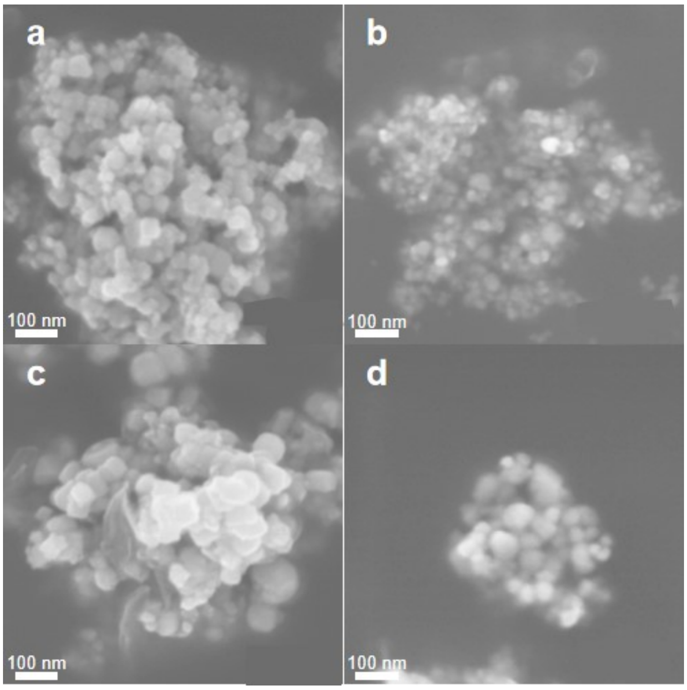

Figure S2 SEM images of $CuRh_1Cr_1$ DMSC and comparative samples. a) $CuRh_1Cr_1$ DMSC. b) $CuRh_1$ MSC. c) $CuCr_1$ MSC. d) Cu.

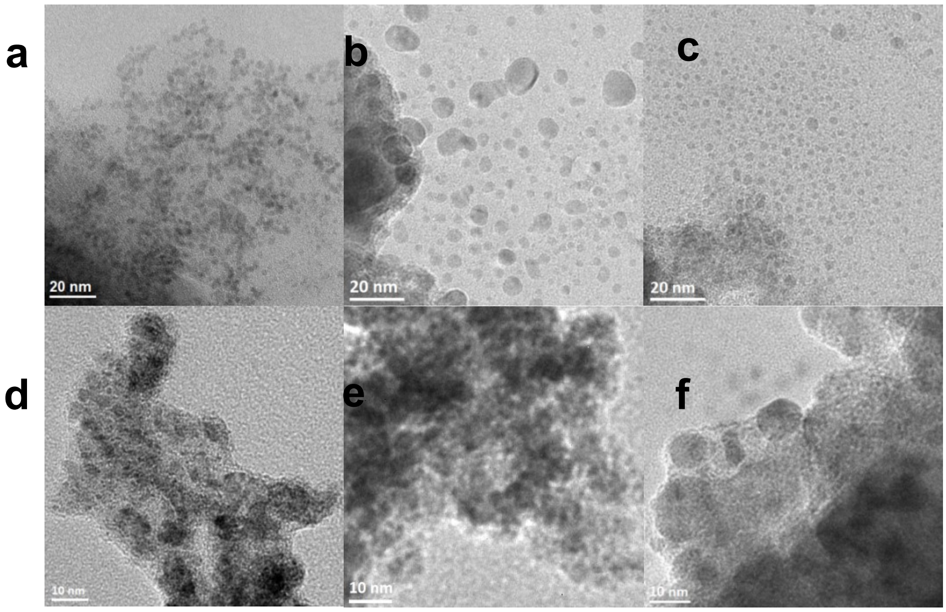

Figure S3 TEM images of $CuRh_1Cr_1$ DMSC and comparative samples. a) Low-resolution TEM image of dispersed particles of $CuRh_1Cr_1$ DMSC. b) Low-resolution TEM image of dispersed particles of $CuRh_1$ MSC. c) Low-resolution TEM image of dispersed particles of $CuCr_1$ MSC. d) High-resolution TEM image of particle aggregates of $CuRh_1Cr_1$ DMSC. e) High-resolution TEM image of particle aggregates of $CuRh_1$ MSC. f) High-resolution TEM image of particle aggregates of $CuCr_1$ MSC.

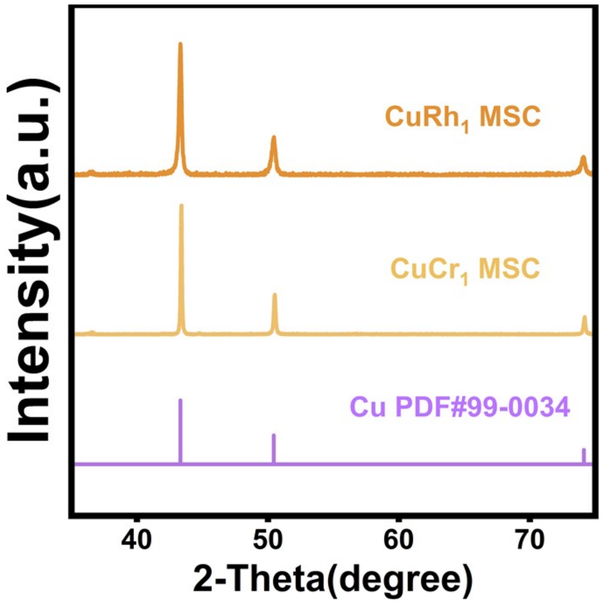

Figure S4 XRD patterns of $CuRh_1$ MSC and $CuCr_1$ MSC.

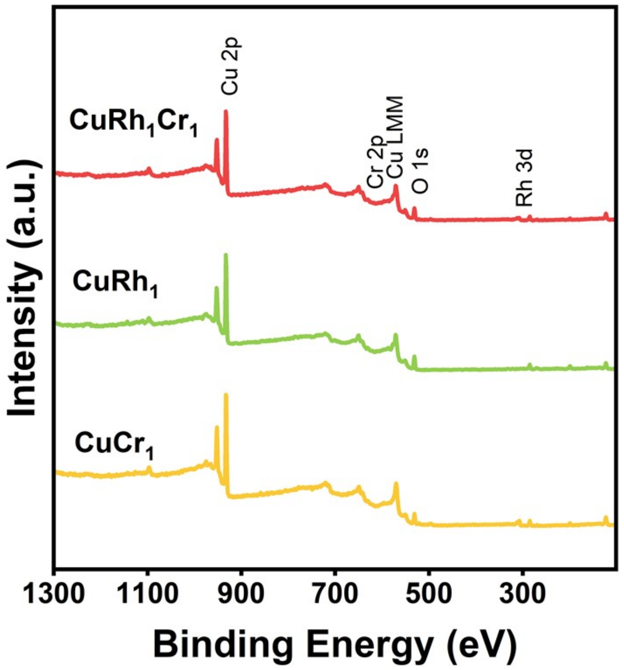

Figure S5 The full XPS spectra of $CuRh_1Cr_1$ DMSC and the reference sample

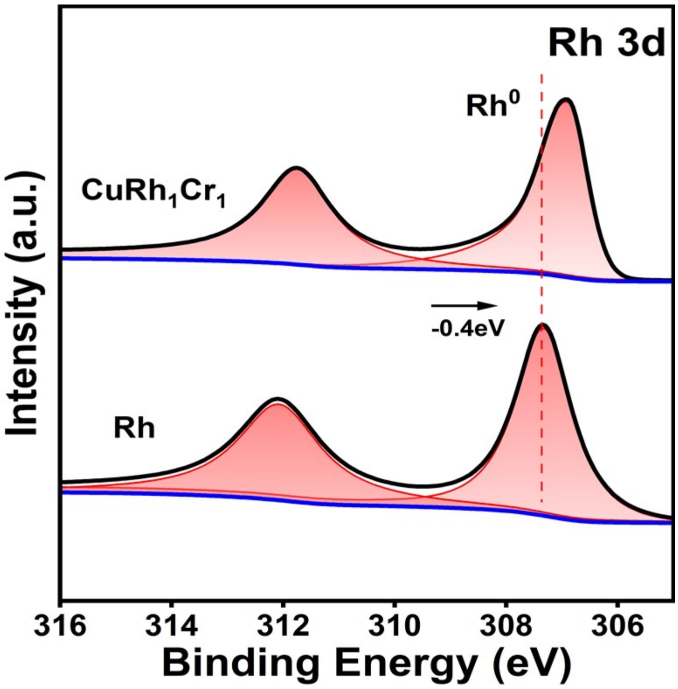

Figure S6 Rh 3d XPS spectra of CuRh$_1$ MSC and Metallic Rh

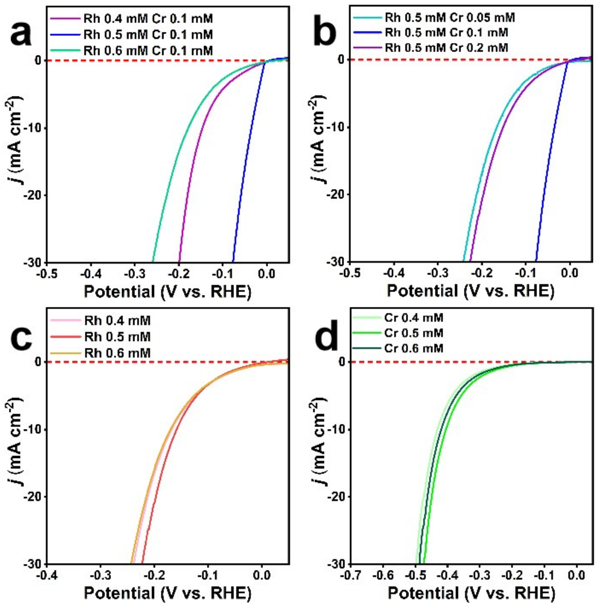

Figure S7 CuRh$_1$Cr$_1$ DMSC and comparison sample concentration gradient orthogonal experiment LSV test. a)b) CuRh$_1$Cr$_1$ DMSC, c) CuRh$_1$ MSC, d) CuCr$_1$ MSC.

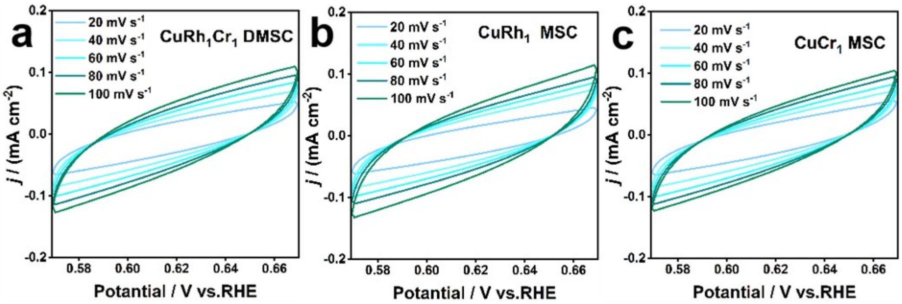

Figure S8 CuRh$_1$Cr$_1$ DMSC and comparison sample ECSA test.

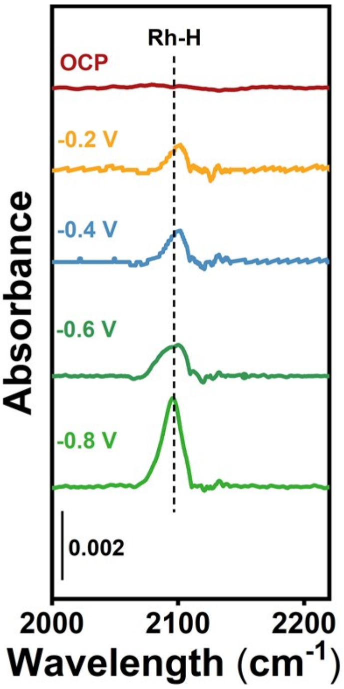

Figure S9 In-situ infrared testing of CuRh$_1$ MSC at different reduction potentials.

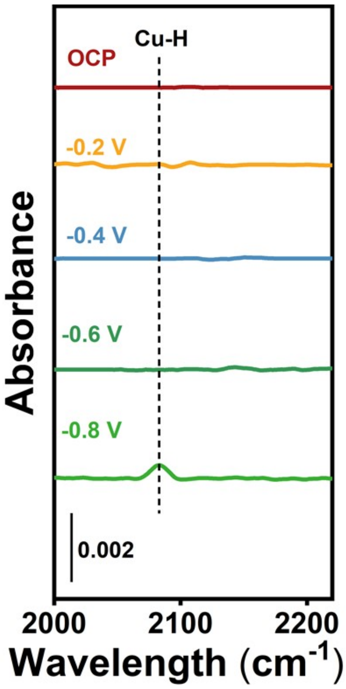

Figure S10 In-situ infrared testing of $CuCr_1$ MSC at different reduction potentials.

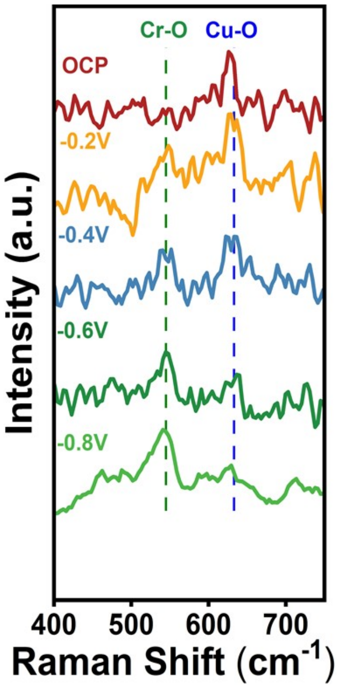

Figure S11 In-situ Raman testing of $CuCr_1$ MSC at different reduction potentials.

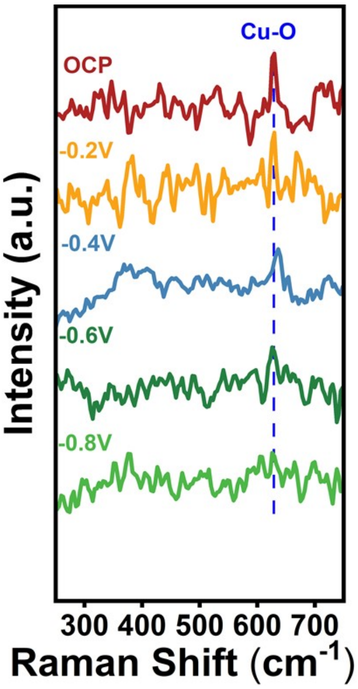

Figure S12 In-situ Raman testing of $CuRh_1$ MSC at different reduction potentials.

Table S1 ICP-MS test results of elemental composition in $CuRh_1Cr_1$ DMSC.

Tested Elements	Test solution element concentration C_0 (mmol/L)	Content at%
Cr	5.668	0.46 at%
Cu	1196	96.02 at%
Rh	43.89	3.52 at%